SCIENTIFIC REPORTS

OPEN

SUBJECT AREAS:
MOLECULAR EVOLUTION
CELL DEATH AND IMMUNE RESPONSE
PROTEIN STRUCTURE PREDICTIONS
CELLULAR SIGNALLING NETWORKS

Received
11 September 2014

Accepted
21 November 2014

Published
11 December 2014

Correspondence and requests for materials should be addressed to A.V.K. (andrey.kajava@crbm.cnrs.fr) or K.H. (kay.hofmann@uni-koeln.de)

# Evolutionary link between metazoan RHIM motif and prion-forming domain of fungal heterokaryon incompatibility factor HET-s/HET-s

Andrey V. Kajava[1,2,3], Karsten Klopffleisch[4], Shuhua Chen[4] & Kay Hofmann[4]

[1]Centre de Recherches de Biochimie Macromoléculaire, CNRS- UMR 5237, 1919 Route de Mende, 34293 Montpellier, Cedex 5, France, [2]Institut de Biologie Computationnelle, 860 rue St Priest, 34095 Montpellier Cedex 5, France, [3]University ITMO, 49 Kronverksky av. 197101 St Petersburg, Russia, [4]Institute for Genetics, University of Cologne, Zülpicher Strasse 47a, D- 50674 Cologne, Germany.

**The Rip homotypic interaction motif (RHIM) is a short, non-globular sequence stretch that mediates a key interaction of mammalian necroptosis signaling. In order to understand its unusual oligomerization properties, we set out to trace the evolutionary origins of the RHIM motif by identifying distantly related protein motifs that might employ the same binding mode. The RHIM motif was found to be related to the prion-forming domain of the HET-s protein, which oligomerizes by forming structurally well-characterized fibrils and is involved in fungal heterokaryon incompatibility. This evolutionary relationship explains the recently reported propensity of mammalian RHIM motifs to form amyloid fibrils, but suggests that these fibrils have a different structural architecture than currently assumed. These findings, together with numerous observations of RHIM-like motifs in immunity proteins from a wide range of species, provide insight to the modern innate immunity pathways in animals, plants and fungi.**

The regulation of cell death in response to viral infection or extracellular factors is of crucial importance for the life of multicellular organisms. Failure to respond properly to death-inducing stimuli can lead to a wide range of diseases, including tumor formation, immunodeficiency, or autoimmune responses. An important death-inducing stimulus is tumor necrosis factor (TNF) and related cytokines. Depending on the circumstances, engagement of the type I TNF receptor by its ligand can lead to three different cellular outcomes: induction of apoptosis, activation of the survival-promoting transcription factor NF-κB, or induction of programmed necrosis (necroptosis). A crucial component of all three TNF-response pathways is the protein kinase RIP1, which together with the proteins TRADD, TRAF2, TRAF5 and cIAP2 forms the TNF-receptor associated complex I. Lys-63 linked polyubiquitination of RIP1 induces NF-κB activation, while RIP1 deubiquitination either leads to caspase-8 dependent apoptosis, or – failing that – to caspase-8 independent necroptosis[1].

The downstream events of the necroptosis pathway are insufficiently understood. In the absence of active caspase-8, RIP1 forms a complex termed 'necrosome' with the related protein kinase RIP3. This hetero-dimerization requires the kinase activity of RIP1 and is mediated by a sequence region called RHIM (for RIP homotypic interaction motif)[2]. Two additional proteins, MLKL (mixed lineage kinase domain-like) and PGAM5 (phosphoglycerate mutase family member 5) have been implicated in the induction of necroptosis downstream of the necrosome, although the mechanistic details remain unresolved[3–5]. Besides RIP1 and RIP3, two copies of the RHIM motif have been found in the double-stranded RNA and Z-DNA binding protein DAI/ZBP1[6,7]. This protein does not participate in the TNF pathway but mediates virus-induced necrosis via a RHIM-mediated recruitment of RIP3. Cytomegaloviruses, in turn, encode a RHIM-containing protein called vIRA, which interferes with RIP3 recruitment by DAI1 and thus helps the virus to evade the necroptosis pathway[8,9].

As a homotypic interaction region, the RHIM motif is highly unusual in that it spans less than 25 residues and is predicted to be unstructured in solution. Usually, protein interactions require at least one folded domain. Recently, it was reported that the RHIM-motifs of RIP1 and RIP3 mediate assembly of these kinases into the amyloid fibrils[10]. To gain a better insight into this issue, we set out to trace the evolutionary origins of the RHIM motif by identifying distantly related protein pairs that might employ the same binding mode. In the first step, we

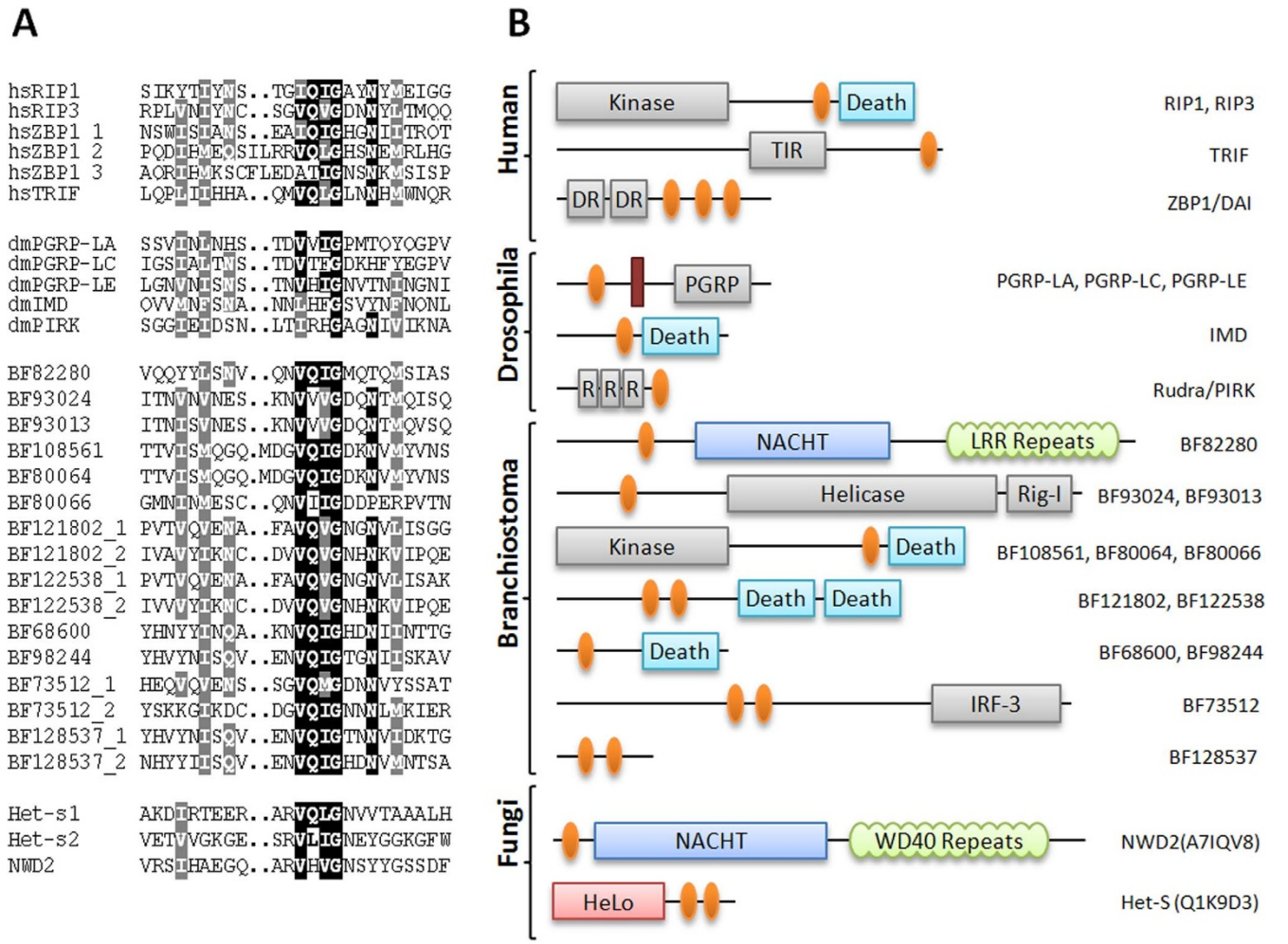


**Figure 1** | **Proteins with RHIM-related motifs.** (A): multiple sequence alignment of representative RHIM domains of human (hs), drosophila (dm), and branchiostoma (BF) proteins and prion-forming domain of *P. anserina* protein. Human and drosophila proteins are denoted by their gene names, branchiostoma proteins by their genome ORF number. Residues invariant or conservatively replaced in at least 50% of all sequences are shown on black and grey background, respectively. (B): Domain architecture of the same proteins, RHIM domains are shown in orange, NACHT-type ATPase domains in blue, death domains in cyan, repeat domains in green, transmembrane region in brown and all other domains in grey.

found divergent RHIM motifs in several invertebrate genomes, including a group of insect proteins that regulate the IMD pathway of innate anti-bacterial immunity. By extending the searches through sensitive bioinformatical sequence comparison methods, we could establish a relationship between the RHIM motif and the prion-forming portion of the HET-s protein of *Podospora anserina* and related fungi[11]. The HET-s protein is a key regulator of a fungal cell death pathway termed 'heterokaryon incompatibility', which in turn is most likely derived from an ancient fungal immunity system[12].

Based on the structurally characterized HET-s prion, we predict a homologous amyloidogenic fold for the RHIM motif. Our model is in agreement with a recent data showing that the RIP1-RIP3 necrosome forms an amyloid-like filament[10]. However, the relationship to the HET-s prion-forming domain (PFD) suggests a different fibril arrangement of the RIP1 and RIP3 portions as compared to the previously published models.

## Results

**The RHIM motif is related to a fungal prion-forming domain.** A generalized sequence profile[13] was constructed from a multiple alignment of established RHIM instances in mammals (RIP1, RIP3, TRIF and ZBP1/DAI relatives) and cytomegaloviruses (vIRA). Database searches identified highly significant matches ($p < 0.01$) to RIP, TRIF and ZBP1-like proteins from other vertebrates, as well as a number of different proteins from fishes and invertebrates. Of particular interest was the identification of a surprisingly large and heterogeneous group of RHIM proteins in the genome of *Branchiostoma floridae*, a recently sequenced cephalochordate[14]. All *Branchiostoma* RHIM proteins have a domain architecture suggesting a role in innate immunity (Fig. 1). Within these proteins, the RHIM is found at positions usually occupied by other interaction domains typically belonging to the CARD-related six-helix family[15]. Several other invertebrates encode subsets of those RHIM families, whereas some lineages (e.g. the tunicates) appear to lack RHIMs altogether.

Insects also encode proteins with RHIM-like motifs, which have a slightly different motif consensus (Fig. 1A). Interestingly, all drosophila RHIM proteins act in the IMD pathway of antibacterial immunity. RHIM motifs were found in the cytoplasmic portion of peptidoglycan receptors PGRP-LA, PGRP-LC, and PGRP-LE, and in the downstream component IMD, which is related to the mammalian RIP1/3 kinases. Surprisingly, although the PGRP receptors bind to IMD, this interaction has been reported not to depend on the RHIM-like motifs[16]. By contrast, the RHIM motifs in the PGRPs are essential for receptor oligomerization and downstream signaling and are also important for the interaction with the IMD pathway inhibitor Rudra/Pirk[16–18]. Like the PGRP and IMD proteins, Rudra/Pirk was also found to harbor a RHIM-like motif at the C-terminus, while

the middle part consists of several copies of an 18-residue repeat that also resembles the C-terminal half of the RHIM motif.

Due to the small size and high divergence of the RHIM motif, the RHIM alignment used for the sequence profile searches is relatively information-poor and the profile-based evaluation of sequence relatedness lacks in statistical power, i.e. the ability to identify all genuine RHIM motifs. We therefore extended the bioinformatical database searches by using the HHsearch method, which compares two Hidden Markov Models (HMMs), each of them derived from a multiple alignment of a sequence family[19]. Through the consideration of family-specific sequence conservation on both sides of the comparison, the sensitivity of the HHsearch method is superior to a simple profile-to-sequence comparison. While profile searches work on a simple protein database, the HHsearch method searches a collection of pre-calculated alignments. In the present case, the searchable alignment collection was based on a set of curated alignments from the Pfam database, augmented by a collection of about 2500 unpublished alignments generated by the authors.

When running HHsearch with an HMM derived from animal RHIM motifs as described in the previous paragraph, there was only one sequence family yielding highly significant scores: the so-called 'prion-forming domain' (PFD) of the HET-s protein in *Podospora anserina* and related filamentous fungi. The PFD of HET-s comprises a tandem repeat of 26 residues[11]; a single copy of this repeat is found in the neighboring gene NWD2[20] (Fig. 1). A Hidden Markov Model of the fungal repeat copies scored with a p-value of $1*10^{-6}$ against a RHIM-derived HMM and was the best non-RHIM match by a margin of at least two orders of magnitude. Conversely, a RHIM-derived HMM was found in the reciprocal PFD-based search with a similar p-value and constituted the best non-PFD match by two orders of magnitude. Besides the bidirectional statistical support from the sequence comparison, the relationship between the RHIM motif and the HET-s PFD is also supported by functional similarities: Like the RHIM, the repeats of the PFD work as homomeric interaction motifs[11] in a pathway leading to cell death.

**Additional similarities between proteins with the RHIM motif and HET-s PFD.** The functional conservation of a RHIM-related motif in animal and fungal death-inducing proteins suggests that there might be further similarities shared between them. Indeed, both RHIM-motifs and HET-s PFDs are flanked by unstructured regions. Furthermore, similar to the HET-s PFDs, the RHIMs sometimes occur as a tandem array of two-three copies. For example, the cytoplasmic DNA sensor ZBP1/DAI and several invertebrate proteins have two or three RHIM motifs linked by long natively unfolded regions[6,7] – similar to the situation found in HET-s fibrils[21].

Moreover, the domain architecture of fungal NWD2 resembles animal APAF1 and NLR proteins (Fig. 1). In the fungal kingdom, several NOD-like STAND receptor proteins have an evolutionary conserved domain architecture: N-terminal PFD, followed by a central nucleotide binding oligomerization domain of the NACHT type and C-terminal ligand binding domain composed of tandem repeats as WD, TPR, ANK or HEAT repeats[20]. Similar domain architecture was found in the animal RHIM-containing proteins, in particular that of branchiostoma BF82280 (Fig. 1).

**A molecular model for RHIM-based amyloid fibrils.** The evolutionary relationship between RHIM and the HET-s prion forming domain – as proposed by bioinformatical methods – has interesting biological implications. Unlike the RHIM-interaction, the PFD-based interactions have been characterized at the molecular level, including a medium-resolution solid state NMR structure[21]. The 3D structure of the HET-s prion fibril provides opportunity on the one hand to verify the match between RHIM and HET-s sequences and on the other hand to get insight into possible 3D structure of RIP1-RIP3 amyloid fibrils. The 3D structure of HET-s prion fibrils represents axial stacking of two-coil β-solenoids each belonging to one HET-s molecule[21]. The two coils are formed by tandemly repeated, similar but not identical sequence motifs. Each coil has two central β-strands (β2 and β3) forming so called β-arch[22] and two short β-strands (β1 and β4) flanking this β-arch (Fig. 2). The stacks of the β-arches build up the β-arcade which represents the core structural element of many known amyloid and prion fibrils formed in vivo. The HET-s β-arcade is sealed by two flanking β-sheets and is surrounded by unstructured N- and C-terminal fragments.

The interior of the known β-arcade structures may accommodate both apolar residues and uncharged polar Asn and Gln. In such arrangements, the same types of side chains recur in the same positions and are axially nearest neighbours. As a result, the interior consists of either the longitudinal rows of apolar residues or H-bonded ladders of Asn and Gln residues. Polar Ser, Thr, and Cys can also be located inside the β-arcades, especially, within the β-bends (or β-arcs) forming H-bonds with each other and/or with the polypeptide backbone[22–24]. At the same time, uncompensated charged residues of the same sign are not observed in the interior of the β-arcades and, the presence of such residues inside of a suggested structural model is a sign for its rejection[24].

By using the 3D structure of HET-s fibrils as a template, we generated a putative arrangement of RHIM motifs of RIP1 and RIP3 in the amyloid fibril. The similar sequence pattern between HET-s prion and RHIM in 3D structure corresponds to the core β-arcade (Fig. 2). At the same time, the N-terminal motif of the HET-s corresponding to the short flanking β-sheet (β1) is absent in the RHIM motif. In contrast, the RHIM-motif is extended towards the C-terminus and has conserved Asn followed by a variable residue and then by apolar residue. This pattern is typical for β-sheets, suggesting that the RHIM fibrils have long C-terminal β-sheet which folds back to the central β-arcade (Fig. 2) forming so called superpleated β-structure[25]. Similar to the HET-s prion forming region, the RHIM-motif is flanked by unstructured regions.

Our analysis suggests that RHIM fibrils are similar to the HET-s fibrils in the central β-arcade region and have some difference at the flanking regions. It is worth mentioning that in the HET-s fibrils two differing but related motifs (HET-s1 and 2) a linked covalently and, therefore, alternate along the fibril. However, the RHIM-motifs of RIP1 and RIP3 are not covalently linked and, in principle, may allow different RIP1-RIP3 stoichiometries in the fibrils.

The proposed structural arrangement of RIP1/RIP3 fibrils is in agreement with recent experimental study demonstrated formation of the cross-β amyloid fibrils by RIP1 and RIP3 proteins via the RHIM motif[10]. It was shown that the shortest fragments able to retain RIP1/RIP3 interaction are 31 residues (525–555) for RIP1 and 19 residues (446–464) for RIP3. These fragments contain regions which, in accordance with our models, are essential for fibril-formation (Fig. 2). The solid-state NMR data can be explained by about 37 ordered residues of RIP1/RIP3 complex that corresponds to the number of residues in the core of our model. Furthermore, both NMR study and mutational analysis showed that the GIQIGA and GVQVGD motifs of RIP1 and RIP3, respectively, are the most important structural element of the fibril. In line with these data, our model predicts these motifs as the central and most buried region of the structure. The NMR measurements also identified a few non-β-structured residues located within the predicted loop-region. In the HET-s fibril structure and in our model of RIP1/RIP3 fibrils, a strictly conserved Gly (Fig. 2A) plays a critical role in the formation of a sharp turn that stops the extension of a β-strand. Mutations of this Gly in both cases block the fibril formation[10,26]. Finally, it was demonstrated that the RIP1, RIP3 and RIP1/RIP3 fibrils can efficiently cross-seed each other suggesting their similar structural arrangement[10]. Indeed, our model predicts a similar structure of the growing-tips, which could explain these experimental findings.

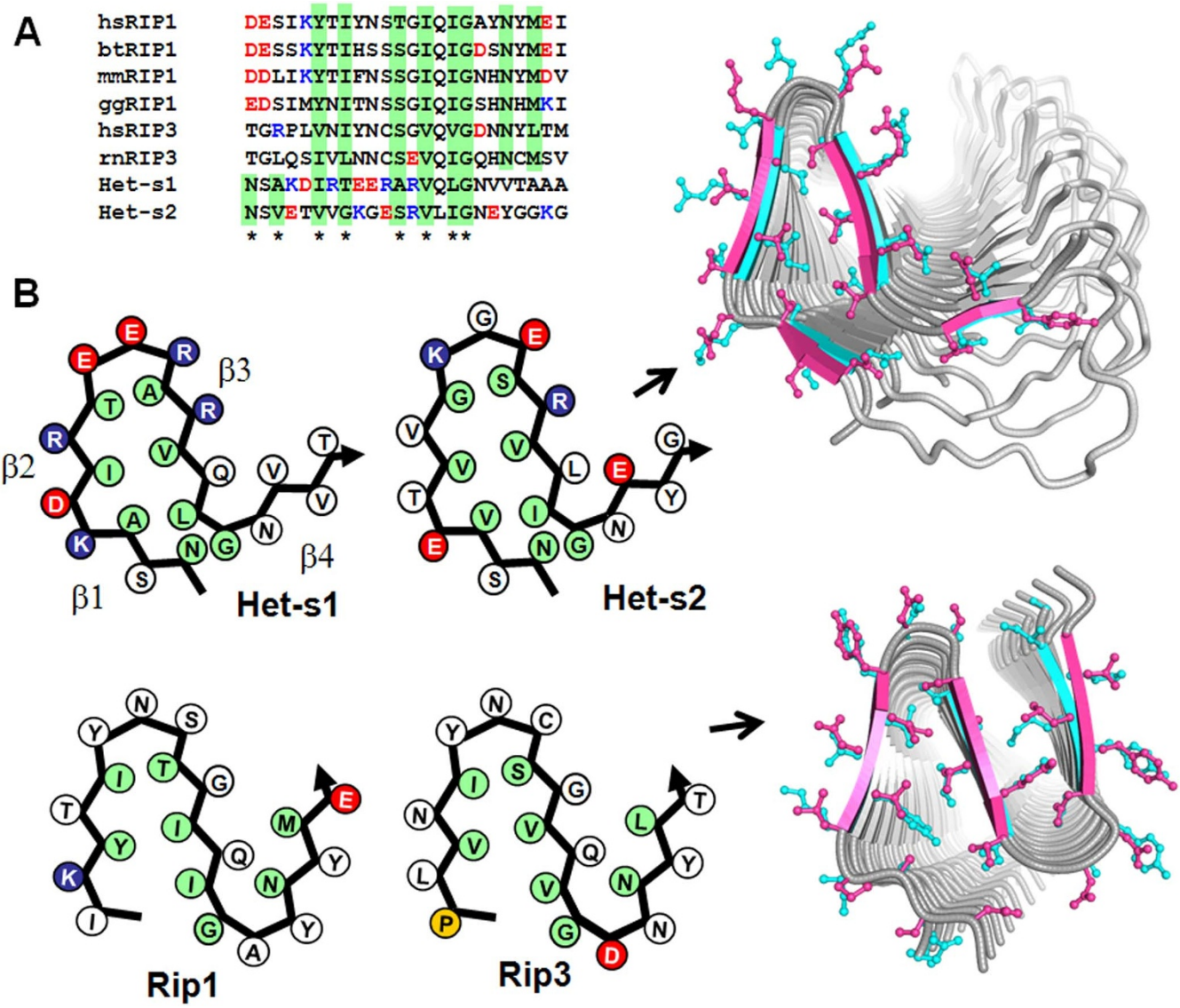


**Figure 2 | Similarity between RHIM motif and HET-s PFD.** (A): Sequence alignment of representative RHIM motifs from RIP1 and RIP3 proteins and two repeats from prion-forming domain of *P. anserina* HET-S protein. Asterisks indicate the hydrophobic core positions of the HET-s amyloid. Columns of similar residues assumed to be inside the amyloid fibrils are printed on green background. Negatively or positively charged residues, which are usually located outside of the fibrils, are printed in red and blue, respectively. (B): Schematic representation of two coils of the β-solenoid core structure of HET-s (top) and two layers of a structural model of the RIP1/RIP3 fibrils (bottom). Side chains are shown as circles color-coded as in the alignment shown in panel A. The rightmost part shows the 3D structure of a HET-s fibril (pdb:2KJ3, residues 218–289) and a structural model of RIP1/RIP3 fibril viewed along the fibril axis. Two front layers are shown in color (magenta and light blue). The remaining layers are shown in grey with omitted side chains for clarity. β-strands are shown as arrows.

While the rules of amyloid fibril formation dictate that each individual β-arch in a given β-arcade assumes the same structure, it is nevertheless possible that the same sequence can engage in different types of β-arcades – depending on the conditions and seed availability. This polymorphic behavior has been described for certain amyloids[27] but might be more general. In the case of the RHIM motif, the arrangement shown in Fig. 2 might not be the only possible structure, since an alternative core β-arcade has been found (Suppl. Data, Fig. S1) that also fulfills all requirements of amyloidogenicity[24]. Both possible arrangements need to be considered in a model-based interpretation of experimental data or for the design of future experiments.

## Discussion

The newly discovered evolutionary relationship between the metazoan RHIM motif and the prion-forming domain of the fungal heterokaryon incompatibility factor HET-s/HET-s is of particular interest since it suggests a novel signaling mechanism based on induced formation of amyloid structures. Our initial prediction of an amyloid-forming role of the RHIM, based on the analogy to the fungal HET-s counterpart[21], has recently been confirmed experimentally by directly demonstrating RHIM-based amyloid fibrils[10]. However, our evolution-based amyloid model differs in fibril architecture and mode of initiation from the model put forward in the previous study. The analogy to the HET-s PFD amyloid suggests a stacking of RIP1 and RIP3 fibril-forming regions along the fibril axis rather than the side-by-side interaction of RIP1 and RIP3 proposed by (Li et al. 2012). In fact, the other known proteins with the amyloid-forming domains that are linked to globular domain(s) by flexible unfolded regions, such as Sup35p, Ure2p, and HET-s, form single protofibrils. In these proteins, the protofibrils are surrounded by clouds of the globular domains, making them unlikely to be accessible for direct side-by-side interactions[28].

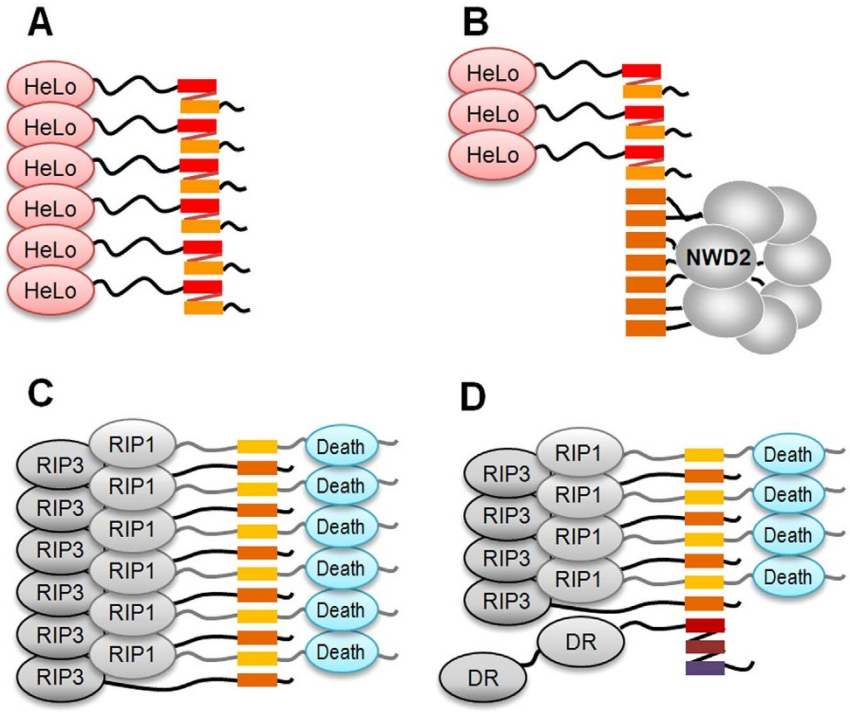


**Figure 3 | Different modes of causing cell death trough amyloid-like oligomerization.** HeLo-like domains are represented as grey bubbles, RHIM-like motifs as boxes of different colors, and other domains as pink, grey and blue bubbles. (A): HeLo clustering in amyloid structure (HET-S), induced during fungal heterokaryon incompatibility. (B): HeLo clustering in amyloid structure (HET-S), induced by triggered NWD2 heptamerization. (C): Mammalian necrosis, induced by binding to a RHIM-mediated amyloid containing RIP1/RIP3 kinases. (D): Mammalian necrosis, induced by binding of the ZBP1/DAI to the RHIM of RIP3 kinase.

For the fibril arrangement of RIP1/RIP3 stacks, two alternative models are conceivable: the fibril-formation might be triggered by one type of protein (e.g. RIP1), followed by an elongation of the pre-formed fibril through the second protein (RIP3). Alternatively, the two proteins might alternate along the fibril axis (Fig. 3). Based on the available data, neither model can be disregarded. However, the presence of charged residues in the amyloid forming regions of several RHIM proteins favors the latter arrangement: in homo-fibrils with parallel and in-register β-structures, residues with charges of the same sign would stack over each other in the adjacent β-strands, resulting in a destabilization through electrostatic repulsion. By contrast, in hetero-fibrils of alternating RIP1 and RIP3 stretches, the increased distance between the charged would alleviate this problem. The posttranslational modification of the amyloidogenic regions, e.g. by introduction or removal of charged moieties, would offer an interesting possibility to regulate the RHIM-based fibril formation.

The reported acetylation of RIP1 at lysine 530, which makes necroptosis dependent on the deacetylase activity of SIRT2, would provide an example for this mechanism[29]. However, the validity of these findings has been recently challenged[30].

Another factor influencing the likelihood of homomeric vs. heteromeric RIP1/RIP3 amyloids is the interplay between the fibril forming region and the RIP1 death-domain, which are connected by a short linker. This situation might lead to steric clashes in a homomeric RIP1 fibril, thus favoring the alternating heteromeric arrangement. On the other hand, death domains are known to mediate homotypic interactions[31] and an arrangement of three or more densely packed death domains might actually help seeding the amyloid rather than preventing it. The resolution of this question will have to await further experimental studies.

The cytoplasmic DNA sensor ZBP1/DAI and several invertebrate proteins have two or three RHIM motifs linked by long natively unfolded regions[6,7]. This arrangement allows the formation of β-solenoid structure consisted of two - three coils corresponding to the consecutive but non-identical RHIMs – similar to the situation found in HET-s fibrils[21]. The covalent linkage of multiple RHIMs should be advantageous for the amyloid seed formation. The non-identical β-solenoid coils can also avoid the stacking of same-charge residues, or even favor fibril induction by stacking opposite-charge residues. The ZBP1/DAI protein was identified as a partner of RIP3 kinase and an essential protein for the induction of regulated necrosis in cytomegalovirus-infected cells[7]. Our model suggests that the β-solenoid of RHIMs from ZBP1/DAI can trigger RIP1/RIP3 amyloid formation by interaction with the RHIM of RIP3 (Fig. 3). In its turn, to disrupt this ZBP1/DAI and RIP3 interaction, cytomegaloviruses can use their RHIM containing inhibitors vIRA[32].

The fungal STAND ATPase NWD2 has a PFD/RHIM-like motif at its effector end and has been proposed to initiate an amyloid fibril upon heptamerization[20]. This amyloid could be extended by HET-s in a conventional linear fashion[20], but a heptameric arrangement of HET-s molecules bound to an activated NWD2 heptamer is also conceivable (Fig. 3).

## Methods

**Sequence analysis.** All sequence database searches were performed with a nonredundant data set constructed from the current release of UNIPROT[33], combined with a number of species-specific protein databases for fungi, plants, and invertebrates. The latter databases were downloaded from the web pages of the respective sequencing projects at the Broad Institute of Harvard and MIT (http://www.broad.mit.edu) and the DOE joint Genome Institute (http://www.jgi.doe.gov) using the PHYTOZOME and MYCOCOSM portals[34,35]. Sequence database searches were performed by the generalized profile method[13], using the *pftools* package[36]. Generalized profiles were constructed using the BLOSUM45 substitution matrix and default penalties of 2.1 for gap opening and 0.2 for gap extension. The statistical significance of profile matches was derived from the analysis of the score distribution of a randomized database[37]. Only sequence matches found with a probability of $p < 0.01$ were included into subsequent rounds of iterative profile refinement. Highly sensitive database searches were performed by Hidden Markov Model (HMM) to HMM comparisons, using the HHsearch program package[19]. The HMM databases required for this search were generated from three set of multiple alignments, covering orthologous sequence groups of animals, plants and fungi, respectively.

Orthology relationships were established using INPARANOID[38]. Sequences were aligned using the L-ins-I algorithm of the MAFFT package[39].

**Molecular modeling.** Molecular modeling of the 3D structures of RIP1/RIP3 fibrils were performed by using Homology and Discovery modules of Insight II program[40]. The models were further refined by the energy minimization procedure that was based on the steepest descent algorithm (100 steps) followed by the conjugate gradients algorithm (500 steps). The consistent valence force field and the distance dependent dielectric constant were used. Images of molecular structures on Fig. 2 and S1 were generated with Pymol program[41]. Alternative structural arrangements of the RHIM-containing fibrils (Fig. S1) were proposed by the ArchCandy program[24]. To build the molecular models we used templates of the β-arc conformations found in the known structures of β-solenoids[42].


1. Vandenabeele, P., Galluzzi, L., Vanden Berghe, T. & Kroemer, G. Molecular mechanisms of necroptosis: an ordered cellular explosion. *Nat Rev Mol Cell Biol* **11**, 700–714 (2010).
2. Sun, X., Yin, J., Starovasnik, M. A., Fairbrother, W. J. & Dixit, V. M. Identification of a novel homotypic interaction motif required for the phosphorylation of receptor-interacting protein (RIP) by RIP3. *J Biol Chem* **277**, 9505–9511 (2002).
3. Sun, L. *et al*. Mixed lineage kinase domain-like protein mediates necrosis signaling downstream of RIP3 kinase. *Cell* **148**, 213–227 (2012).
4. Wang, Z., Jiang, H., Chen, S., Du, F. & Wang, X. The mitochondrial phosphatase PGAM5 functions at the convergence point of multiple necrotic death pathways. *Cell* **148**, 228–243 (2012).
5. Zhao, J. *et al*. Mixed lineage kinase domain-like is a key receptor interacting protein 3 downstream component of TNF-induced necrosis. *Proc Natl Acad Sci U S A* **109**, 5322–5327 (2012).
6. Rebsamen, M. *et al*. DAI/ZBP1 recruits RIP1 and RIP3 through RIP homotypic interaction motifs to activate NF-kappaB. *EMBO Rep* **10**, 916–922 (2009).
7. Upton, J. W., Kaiser, W. J. & Mocarski, E. S. DAI/ZBP1/DLM-1 complexes with RIP3 to mediate virus-induced programmed necrosis that is targeted by murine cytomegalovirus vIRA. *Cell Host Microbe* **11**, 290–297 (2012).
8. Upton, J. W., Kaiser, W. J. & Mocarski, E. S. Cytomegalovirus M45 cell death suppression requires receptor-interacting protein (RIP) homotypic interaction motif (RHIM)-dependent interaction with RIP1. *J Biol Chem* **283**, 16966–16970 (2008).
9. Upton, J. W., Kaiser, W. J. & Mocarski, E. S. Virus inhibition of RIP3-dependent necrosis. *Cell Host Microbe* **7**, 302–313 (2010).
10. Li, J. *et al*. The RIP1/RIP3 necrosome forms a functional amyloid signaling complex required for programmed necrosis. *Cell* **150**, 339–350 (2012).
11. Ritter, C. *et al*. Correlation of structural elements and infectivity of the HET-s prion. *Nature* **435**, 844–848 (2005).
12. Saupe, S. J. The [HET-s] prion of Podospora anserina and its role in heterokaryon incompatibility. *Semin Cell Dev Biol* **22**, 460–468 (2011).
13. Bucher, P., Karplus, K., Moeri, N. & Hofmann, K. A flexible motif search technique based on generalized profiles. *Comput Chem* **20**, 3–23 (1996).
14. Putnam, N. H. *et al*. The amphioxus genome and the evolution of the chordate karyotype. *Nature* **453**, 1064–1071 (2008).
15. Hofmann, K., Bucher, P. & Tschopp, J. The CARD domain: a new apoptotic signalling motif. *Trends Biochem Sci* **22**, 155–156 (1997).
16. Kaneko, T. *et al*. PGRP-LC and PGRP-LE have essential yet distinct functions in the drosophila immune response to monomeric DAP-type peptidoglycan. *Nat Immunol* **7**, 715–723 (2006).
17. Aggarwal, K. *et al*. Rudra interrupts receptor signaling complexes to negatively regulate the IMD pathway. *PLoS Pathog* **4**, e1000120 (2008).
18. Kleino, A. *et al*. Pirk is a negative regulator of the Drosophila Imd pathway. *J Immunol* **180**, 5413–5422 (2008).
19. Soding, J. Protein homology detection by HMM-HMM comparison. *Bioinformatics* **21**, 951–960 (2005).
20. Daskalov, A., Paoletti, M., Ness, F. & Saupe, S. J. Genomic clustering and homology between HET-s and the NWD2 STAND protein in various fungal genomes. *PLoS One* **7**, e34854 (2012).
21. Wasmer, C. *et al*. Amyloid fibrils of the HET-s(218-289) prion form a beta solenoid with a triangular hydrophobic core. *Science* **319**, 1523–1526 (2008).
22. Kajava, A. V., Baxa, U. & Steven, A. C. Beta arcades: recurring motifs in naturally occurring and disease-related amyloid fibrils. *FASEB J* **24**, 1311–1319 (2010).
23. Kajava, A. V. & Steven, A. C. Beta-rolls, beta-helices, and other beta-solenoid proteins. *Adv Protein Chem* **73**, 55–96 (2006).
24. Ahmed, A. B., Znassi, N., Chateau, M. T. & Kajava, A. V. A structure-based approach to predict predisposition to amyloidosis. *Alzheimers Dement* (2014).
25. Kajava, A. V., Baxa, U., Wickner, R. B. & Steven, A. C. A model for Ure2p prion filaments and other amyloids: the parallel superpleated beta-structure. *Proc Natl Acad Sci U S A* **101**, 7885–7890 (2004).
26. Daskalov, A. *et al*. Contribution of specific residues of the beta-solenoid fold to HET-s prion function, amyloid structure and stability. *PLoS Pathog* **10**, e1004158 (2014).
27. Diaz-Avalos, R., King, C. Y., Wall, J., Simon, M. & Caspar, D. L. Strain-specific morphologies of yeast prion amyloid fibrils. *Proc Natl Acad Sci U S A* **102**, 10165–10170 (2005).
28. Baxa, U., Keller, P. W., Cheng, N., Wall, J. S. & Steven, A. C. In Sup35p filaments (the [PSI+] prion), the globular C-terminal domains are widely offset from the amyloid fibril backbone. *Mol Microbiol* **79**, 523–532 (2011).
29. Narayan, N. *et al*. The NAD-dependent deacetylase SIRT2 is required for programmed necrosis. *Nature* **492**, 199–204 (2012).
30. Newton, K. *et al*. Is SIRT2 required for necroptosis? *Nature* **506**, E4–6 (2014).
31. Park, H. H. *et al*. The death domain superfamily in intracellular signaling of apoptosis and inflammation. *Annu Rev Immunol* **25**, 561–586 (2007).
32. Mocarski, E. S., Upton, J. W. & Kaiser, W. J. Viral infection and the evolution of caspase 8-regulated apoptotic and necrotic death pathways. *Nat Rev Immunol* **12**, 79–88 (2012).
33. Magrane, M. & Consortium, U. UniProt Knowledgebase: a hub of integrated protein data. *Database (Oxford)* **2011**, bar009 (2011).
34. Goodstein, D. M. *et al*. Phytozome: a comparative platform for green plant genomics. *Nucleic Acids Res* **40**, D1178–1186 (2012).
35. Grigoriev, I. V. *et al*. The genome portal of the Department of Energy Joint Genome Institute. *Nucleic Acids Res* **40**, D26–32 (2012).
36. Schuepbach, T. *et al*. pfsearchV3: a code acceleration and heuristic to search PROSITE profiles. *Bioinformatics* **29**, 1215–1217 (2013).
37. Hofmann, K. Sensitive protein comparisons with profiles and hidden Markov models. *Brief Bioinform* **1**, 167–178 (2000).
38. Ostlund, G. *et al*. InParanoid 7: new algorithms and tools for eukaryotic orthology analysis. *Nucleic Acids Res* **38**, D196–203 (2010).
39. Katoh, K. & Standley, D. M. MAFFT multiple sequence alignment software version 7: improvements in performance and usability. *Mol Biol Evol* **30**, 772–780 (2013).
40. Dayringer, H. E., Tramontano, A., Sprang, S. R. & Fletterick, R. J. Interactive program for visualization and modelling of proteins, nucleic acids and small molecules. *J Mol Graph* **4**, 82–87 (1986).
41. DeLano, W. L. The PyMol Molecular Graphics System. DeLano Scientific, San Carlos, CA, USA. (2002).
42. Hennetin, J., Jullian, B., Steven, A. C. & Kajava, A. V. Standard conformations of beta-arches in beta-solenoid proteins. *J Mol Biol* **358**, 1094–1105 (2006).


## Acknowledgments

This work was funded by a grant from the Deutsche Forschungsgemeinschaft (SFB 670) to K.H.

## Author contributions

K.H. initiated the study; K.H., A.V.K. and K.K. performed the sequence analysis; A.V.K. made structural predictions; A.V.K. and K.H. wrote the manuscript; K.K. and S.C. contributed ideas.

## Additional information

**Supplementary information** accompanies this paper at http://www.nature.com/scientificreports

**Competing financial interests:** The authors declare no competing financial interests.

**How to cite this article:** Kajava, A.V., Klopffleisch, K., Chen, S. & Hofmann, K. Evolutionary link between metazoan RHIM motif and prion-forming domain of fungal heterokaryon incompatibility factor HET-s/HET-s. *Sci. Rep.* **4**, 7436; DOI:10.1038/srep07436 (2014).